available at www.sciencedirect.com

ScienceDirect

www.elsevier.com/locate/brainres

BRAIN RESEARCH

Research Report

Acupuncture modulates spontaneous activities in the anticorrelated resting brain networks

Lijun Bai[a], *Wei Qin*[a], *Jie Tian*[a,b,*], *Minghao Dong*[a], *Xiaohong Pan*[e], *Peng Chen*[f], *Jianping Dai*[g], *Wanhai Yang*[h], *Yijun Liu*[c,d,*]

[a]*Life Science Research Center, School of Life Science and Technology, Xidian University, Xi' an, 710071, China*
[b]*Institute of Automation, Chinese Academy of Sciences, Beijing 100190, China*
[c]*Department of Psychiatry, McKnight Brain Institute, University of Florida, Gainesville, FL 32610, USA*
[d]*Department of Neuroscience, McKnight Brain Institute, University of Florida, Gainesville, FL 32610, USA*
[e]*Department of Psychology, School of Education Science, East China Normal University, China*
[f]*Beijing Traditional Chinese Medicine Hospital, Capital Medical University, China*
[g]*Department of Radiology, Beijing Tiantan Hospital, Capital University of Medical Sciences, China*
[h]*Life Science Research Center, School of Electronic Engineering, Xidian University, Xi' an 710071, China*

ARTICLE INFO

Article history:
Accepted 29 April 2009
Available online 8 May 2009

Keywords:
Acupuncture
Insula
Endogenous pain modulation
Spontaneous brain activity
Anticorrelated resting brain network

ABSTRACT

Neuroimaging studies of acupuncture have demonstrated extensive signal attenuations in the core regions of a "default mode" network as well as signal potentiations in the regions of a "central-executive" network. We proposed that this acupuncture-related dichotomy may represent the anticorrelation in these intrinsic brain networks showing spontaneous fluctuations during rest. According to a plentiful clinical report, acupuncture can provide pain relief beyond the time it is being administrated; therefore, imaging its sustained effect (rather than acute effect) on the brain networks may further help elucidate the mechanisms by which acupuncture achieves its therapeutic effects. As an interface, the anterior insula (AI) has recently been shown to be a network hub, which initiates dynamic switching between these intrinsic networks. Here, we attempt to explore how acupuncture can modulate spontaneous coherences of these resting networks anchored by the AI. Using a spontaneous activity detection approach, we identified an AI-related dichotomy showing spontaneous activations in the CEN along with wide spontaneous deactivations located exclusively in the DMN. Following verum acupuncture, but not sham control, there was a

* *Corresponding authors.* J. Tian is to be contacted at the Medical Image Processing Group, Key Laboratory of Complex Systems and Intelligence Science, Institute of Automation, Chinese Academy of Science, P.O. Box 2728, Beijing 100190, China; Life Science Research Center, School of life science and technology, Xidian University, Xi'an, 710071, China. Fax: +86 10 62527995. Y. Liu, Department of Psychiatry, McKnight Brain Institute, University of Florida, 100 Newell Drive, P.O. Box 100256, Gainesville, FL 32610, USA; Department of Neuroscience, McKnight Brain Institute, University of Florida, 100 Newell Drive, P.O. Box 100256, Gainesville, FL 32610, USA. Fax: +1 352 392 3579.
E-mail addresses: tian@ieee.org (J. Tian), yijunliu@ufl.edu (Y. Liu).

Abbreviations: fMRI, functional magnetic resonance imaging; BOLD, blood oxygenation level-dependent; RS, resting state; PARS, post-acupuncture resting state; PSRS, post-sham resting state; ACUP, verum acupuncture; SHAM, sham acupuncture; MASS, MGH acupuncture sensation scale; ROIs, regions of interest; Spon-TPs, time points of spontaneous activity; HMA, head motion amplitudes; DMN, default mode network; CEN, central-executive network; SN, salience network; AI, anterior insula; Amy, amygdala; PH, parahippocampus; Hipp, hippocampus; PRCN, precuneus; IPC, inferior parietal cortex; PCC, posterior cingulate cortex; MPFC, medial prefrontal cortex; dACC, dorsal anterior cingulate cortex; RN, red nucleus; DLPFC, dorsolateral prefrontal cortex; SMA, supplementary motor area; VMPFC, ventromedial prefrontal cortex; MTC, middle temporal cortex; MTL, medial temporal lobe; SII, secondary somatosensory cortex; PPC, posterior parietal cortex; Hyp, hypothalamus; PAG, periaqueductal gray

0006-8993/$ – see front matter.
doi:10.1016/j.brainres.2009.04.056

prominently enhanced dichotomy in the CEN and DMN networks. More importantly, a long-lasting effect of acupuncture could further modulate intrinsic coherences of the wide interoceptive–autonomic areas, including the paralimbic regions and brainstem nuclei. These findings suggested that acupuncture may not only enhance the dichotomy of the anticorrelated resting networks, but also modulate a larger spatio-temporal extent of spontaneous activities in the salient interoceptive–autonomic network, contributing to potential actions in the endogenous pain-modulation circuits and homeostatic control mechanisms.

1. Introduction

Acupuncture has emerged as an important modality of alternative and complementary therapeutic intervention in Western medicine (Diehl, 1999). For example, a promising efficacy of acupuncture has been shown in the treatments of postoperative and chemotherapy nausea and vomiting (Al-Sadi et al., 1997). It has also become a beneficial adjunct for pain management (Birch et al., 2004; Kwon et al., 2006; NIH, 1998). In the last decades, noninvasive functional magnetic resonance imaging (fMRI) technique has opened a "window" into the brain, allowing us to investigate the central physiological functions involved in acupuncture administration.

Converging evidence from fMRI studies has demonstrated that acupuncture stimulation can modulate neural activities in a wide cortico-subcortical network, particularly the limbic system (Fang et al., in press; Hui et al., 2005; Yoo et al., 2004). The limbic regions, critical to the interoceptive function, receive both direct and indirect signals from the internal milieu, and construct composite and dynamic representations of the body's state and generate regulatory signals necessary to maintain the body's homeostasis (Craig, 2002; Craig, 2003). In practice, the well-identified physical effects of acupuncture needling and its purported clinical efficacy also suggest that acupuncture acts in maintaining a homeostatic balance of the internal state within and across multiple brain systems (Beijing, 1980; Mayer, 2000). Although the mode of its central action is still inconclusive, further understanding of how such external intervention interacts with internal regulatory processes may enlighten us to gain an appreciation of the physiological function and integrated mechanisms involved in acupuncture.

Neuroimaging studies of acupuncture have typically demonstrated extensive signal attenuations, mainly distributed in the medial temporal lobe (amygdala, Amy; parahippocampus, PH; hippocampus, Hipp), the posterior cingulate cortex (PCC), the medial prefrontal cortex (MPFC), and a large section of the parietal cortex (precuneus, PRCN; inferior parietal cortex, IPC) (Fang et al., in press; Hui et al., 2005; Wu et al., 1999; Yoo et al., 2004). The spatial distribution of these deactivated regions has a prominent overlap with the core regions in a "default mode" network (DMN), which is mainly present at rest and its activities are strongly reduced during various goal-directed tasks (Raichle et al., 2001). Conversely, the insular cortex and sensorimotor-related areas, consistently give to positive responses after acupuncture stimulation, regardless of acupoint locations or manipulation modes (Hui et al., 2005; Kong et al., 2002; Yoo et al., 2004; Zhang et al., 2003). From this perspective, we propose that this task- or stimulus-related dichotomy, particularly in the acupuncture, may resemble the intrinsic networks showing spontaneous fluctuations in the resting brain (Fox et al., 2005). The analyses of resting-state functional connectivity have shown that the brain is organized into the widespread anticorrelated functional networks: the deactivated DMN supporting basic internal-driven functions, and two coactivated networks — the "central-executive" network (CEN) serving goal-directed "task mode" functions and the "salience" network (SN) underlying interoceptive–autonomic processing (Fox et al., 2005; Greicius et al., 2003; Seeley et al., 2007). In addition, the deactivated regions within the DMN during a variety of cognitive tasks could also be interrupted by externally driven processes (Gusnard et al., 2001).

Since such an alternating interplay of the exogenous and endogenous sources for the central processing is dynamic and complex, another question is raised whether there is a core brain region for supporting the orientation of higher-order executive or organizational processes (Sridharan et al., 2008). A recent fMRI study using chronometric techniques and Granger causality analysis has provided a possible answer that the anterior insula (AI), a key region in the SN, may play an important role in the cognitive control that is related to task switching, particularly in a dynamic switching between the CEN and DMN (Sridharan et al., 2008). The AI has been widely accepted as a relay station integrating the centrally processed sensory information (visceral and autonomic) for its reciprocal connections with multiple brain regions (Mesulam and Mufson, 1982; Mufson and Mesulam, 1982). This region, particularly the right anterior part, also plays a critical role in the interoceptive awareness of both stimulus-induced and stimulus-independent changes in the homeostatic state, which enables us to regulate the organism's current state by initiating appropriate control signals toward the extrapersonal stimuli (Craig, 2002; Critchley et al., 2004).

As aforementioned, the regions modulated by acupuncture stimulus tend to exhibit a salient resemblance with the organization of the anticorrelated networks in the task-free resting brain. At present, however, it is unknown how these resting networks are modulated during the performance of externally somatosensory stimulation (i.e., acupuncture) and what inferences can be made about the physiological processes underlying these changes. While speculative, abundant clinical reports have indicated that acupuncture can provide prolonged analgesia as a therapy for many other diseases and disorders (Beijing, 1980; Han and Terenius, 1982); this analgesic effect may actually peak long after needling administration (Price et al., 1984). In other words, the effect of acupuncture can sustain beyond the needle manipulation period, thereby

modulating the moment-to-moment processes relevant to the post-stimulus resting brain when there is no longer external stimulus (Bai et al., 2009a; Zhang et al., 2009a). Given that the AI serves the hierarchical initiation of cognitive control signals, specifically with respect to the dynamics of switching between the CEN and DMN, the present study attempted to explore how the prolonged effect of acupuncture, even after the needling process terminated, could modulate the operation of these resting brain networks anchored by the AI.

To test this hypothesis, we employed a spontaneous activity detection approach, originally proposed by Hunter et al. (2006), to investigate the intrinsic coherences in the AI during the resting state (RS), post-acupuncture resting state (PARS) and post-sham resting state (PSRS), respectively. By examining episodic signal responses that are statistically similar in their magnitudes to externally evoked activities such as those in fMRI experiments involving tasks, this method can detect the pattern of spontaneous activity underlying specific neuroanatomical systems in the brain.

2. Results

2.1. Results of psychological analysis

The prevalence of these sensations was expressed as the percentage of individuals in the group that reported the given sensations (Fig. 1A). A statistical analysis found no difference between the verum acupuncture (ACUP) and sham acupuncture (SHAM) in regard to the prevalence of these sensations ($P > 0.08$). However, differences did exist with respect to the type of sensations. Numbness (ACUP: 43.4% of subjects; SHAM: 22.1%), fullness (ACUP: 58.9%; SHAM: 21.7%), and soreness (ACUP: 68.3%; SHAM: 23.8%) was found greater for ACUP. The intensity of sensations was expressed as the average score ± SE (Fig. 1B). The levels of sensations were kept low (mild to moderate), and no statistically significant differences occurred in the average sensation intensity between the ACUP (2.4 ± 1.7) and SHAM (2.2 ± 1.9). There was also no

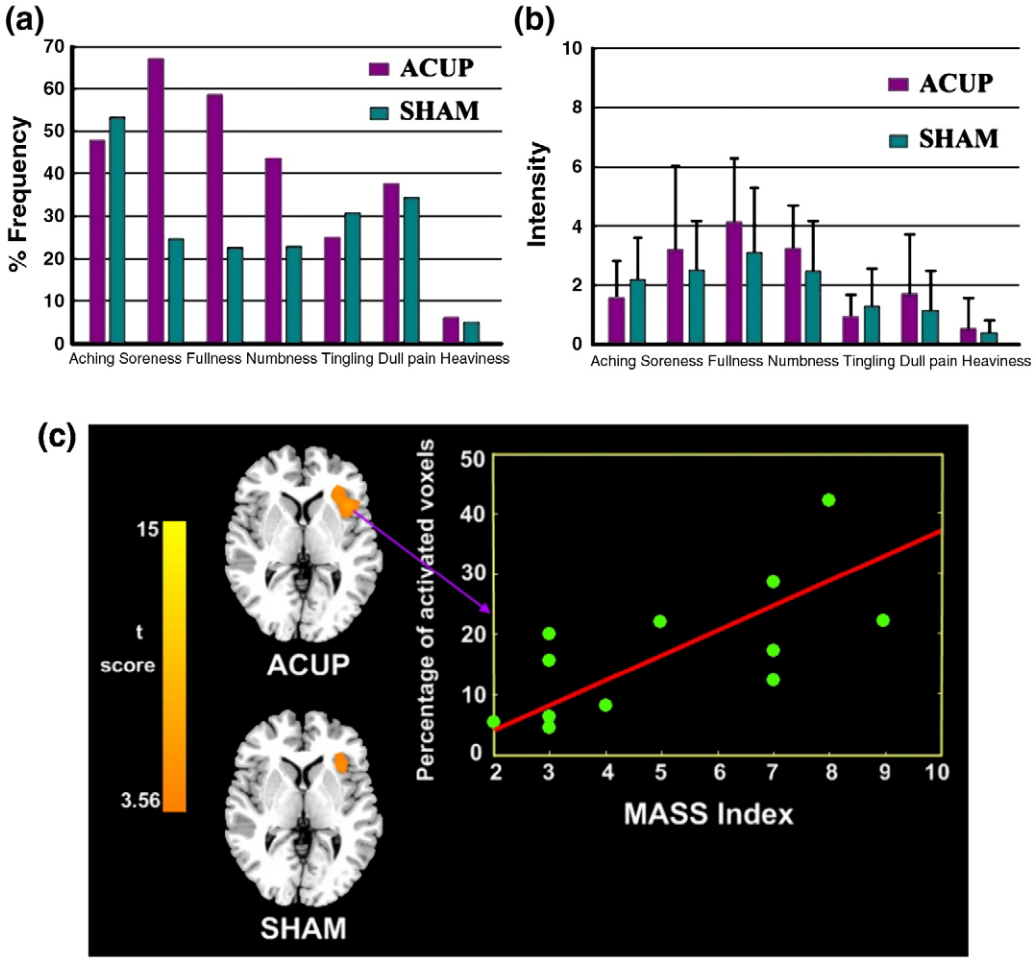

Fig. 1 – Results of psychophysical analysis. A. The percentage of subjects who reported having experienced the given sensation (at least one subject experienced the seven sensations listed). Numbness, fullness, and soreness were found greater for ACUP. B. The intensity of the reported sensations measured by an average score (with standard error bars) on a scale from 0 denoting no sensation to 10 denoting an unbearable sensation. The average stimulus intensities (mean ± SE) were approximately similar during ACUP (2.4 ± 1.7) and SHAM (2.2 ± 1.9). C. Defined ROI (right AI) for spontaneous activity analysis derived from stimulation conditions. Regression plots showed a significant correlation ($r = 0.64$, $P < 0.05$) of the individual *deqi* scores with the activated voxel rate of the right AI, only following the ACUP.

significant difference in the MASS index (an integrated measure of *deqi* intensity, see Experimental procedures) between these two conditions (paired *t*-test, $P>0.05$). Considering a little difference in psychophysical response between the ACUP and SHAM, the neuroimaging findings were likely not the results of differences induced by the sensations.

To examine the relationship between the individual *deqi* sensations and the brain regions activated by the ACUP and SHAM, we also calculated Pearson correlation coefficient between the MASS index and activity extent of the stimulus-related regions (the percentage of activity voxels). Results indicated that the activation rate of the right AI had a high level of correlation with *deqi* scores ($r=0.64$, $P<0.05$) when subjects were receiving the ACUP, but no significant correlation following the SHAM ($P>0.05$) (shown in Fig. 1C). There were no significant correlations for other ROIs in these two conditions. *Deqi* has recently drawn the attention of many scientific researchers, and some studies propose that *deqi* may be important for therapeutic effect (Takeda and Wessel, 1994; Witt et al., 2005). However, systematic testing of the neurobiological basis of *deqi* has still been limited. In this study, we found that individual differences in the *deqi* scores can modulate the degree to which the right AI was activated only following the ACUP. This observation may suggest a key role of the anterior insula in characterizing the central expression of acupuncture stimulation.

2.2. *Spontaneous brain activities in both temporal and spatial domains*

To exclude possible spontaneous activities that are induced by the system noises and subjects' motion, we conducted the following procedures: (i) we determined individually whether more than one time point of spontaneous activity ("Spon-TPs") satisfying $Z>2$ exist in the mean signal of the whole brain (see Experimental procedures). Then we excluded this subject for the further analysis, ensuring that the spontaneous activity from the remained subjects was not derived from the global noise. In this cohort, none were excluded. (ii) To further obviate spontaneous activities derived from the subjects' head motions, we adopted the correlation analysis between the pattern of spontaneous activity and the subjects' head motion amplitudes (HMA). Either the correlation between the HMA of fourteen subjects and the number of their SPon-TPs or the number of their spontaneously active voxels presented no statistical significance, for the PARS ($r=0.02$, $P=0.89$; $r=-0.009$, $P=0.95$), PSRS ($r=0.045$, $P=0.91$; $r=-0.02$, $P=0.87$), and RS ($r=-0.04$, $P=0.76$; $r=-0.015$, $P=0.92$). The same test procedures were also applied to the spontaneous deactivation analysis, resulting in no significant difference ($P>0.05$).

All the subjects demonstrated prominently spontaneous activation/deactivation associated with the right AI during the PARS, PSRS and RS. The mean observed spontaneous activity voxels and the detected time points were presented in Table 1. In addition, the schematic pattern of the spontaneous activity, from a representative subject during the PARS, presented a large proportion (even>35%) of voxels in the right AI with significantly increased ($Z>2$) activity; meanwhile, we detected a total of 6 Spon-TPs, occupying more than 10% of the whole resting time points.

In ACUP condition, the number of voxels contained in the ROI of the right AI was 189. According to Gaussian assumptions, the expected number (mean±SD) of voxels with $Z>2$ could be estimated to be about 4.7±2.9 (corrected for spatial smoothing based on the results of Worsley and Friston, 1995) (Worsley and Friston, 1995). As shown in the Table 1, the mean number of voxels with $Z>2$ in the right AI at spontaneously activated time points was 35.4±9.4 (about 18.7±4.9% of the overall voxels in the ROI). This number exceeded the expectation level (2.5%) and therefore indicated that these spontaneous activations were not random.

2.3. *Spontaneous activities of the right AI network during PARS, PSRS and RS*

During the RS, the right AI showed prominently spontaneous activations associated with the paralimbic and subcortical regions, including the bilateral insula, dorsal anterior cingulate cortex (dACC), thalamus and substantia nigra/red nucleus (RN) ($P<0.005$, FDR corrected, cluster size>10 voxels shown in Fig. 2 and Table 2). This network was referred as a "salience network" underlying interoceptive–autonomic processing and homeostatic functions (Seeley et al., 2007). There were additional AI-related spontaneous activations in the dorsolateral prefrontal cortex (DLPFC) and supplementary motor area (SMA). These CEN-related areas are critical to active maintenance and manipulation for goal-directed judgment and decision (Bunge et al., 2001; Koechlin and Summerfield, 2007). Conversely, the spontaneous deactivation was mainly located in the DMN-related regions, comprising the PCC/PRCN, ventromedial prefrontal cortex (VMPFC), and middle temporal cortex (MTC).

Following the ACUP, these spontaneous activation and deactivation networks anchored by the right AI kept relatively

Table 1 – Characteristics of the spontaneous activation/deactivation in the right AI (*N*=14).

	Right AI		
	PARS	PSRS	RS
Temporal domain (mean±SD)	Activation (deactivation)		
Total time points	50	50	50
Spon-TPs	5.5±1.8 (4.5±1.5)	3.8±1.6 (3.1±1.3)	4.4±1.4 (4.2±1.5)
Percentage of total time points (%)	11±3.6 (9±3)	7.6±3.2 (6.2±2.6)	8.8±2.8 (8.4±3)
Spatial domain (mean±SD)			
Total voxels in ROI	189	189	189
Expected voxels satisfying $Z>2$ ($Z<-2$)	4.7±2.9	4.7±2.9	4.7±2.9
Detected voxels satisfying $Z>2$ ($Z<-2$)	35.4±9.4 (26.5±8.2)	27.0±9.5 (22.8±7)	25.5±7.6 (18.3±5)
Percentage of total voxels (%)	18.7±4.9 (14.0±4.3)	14.3±5.0 (12.1±4)	13.5±4.0 (9.7±2.6)

Note. The expected number of voxels satisfying $Z>2$ or $Z<-2$ has been corrected for the effect arising from the spatial smoothing based on the results of Worsley and Friston (1995).

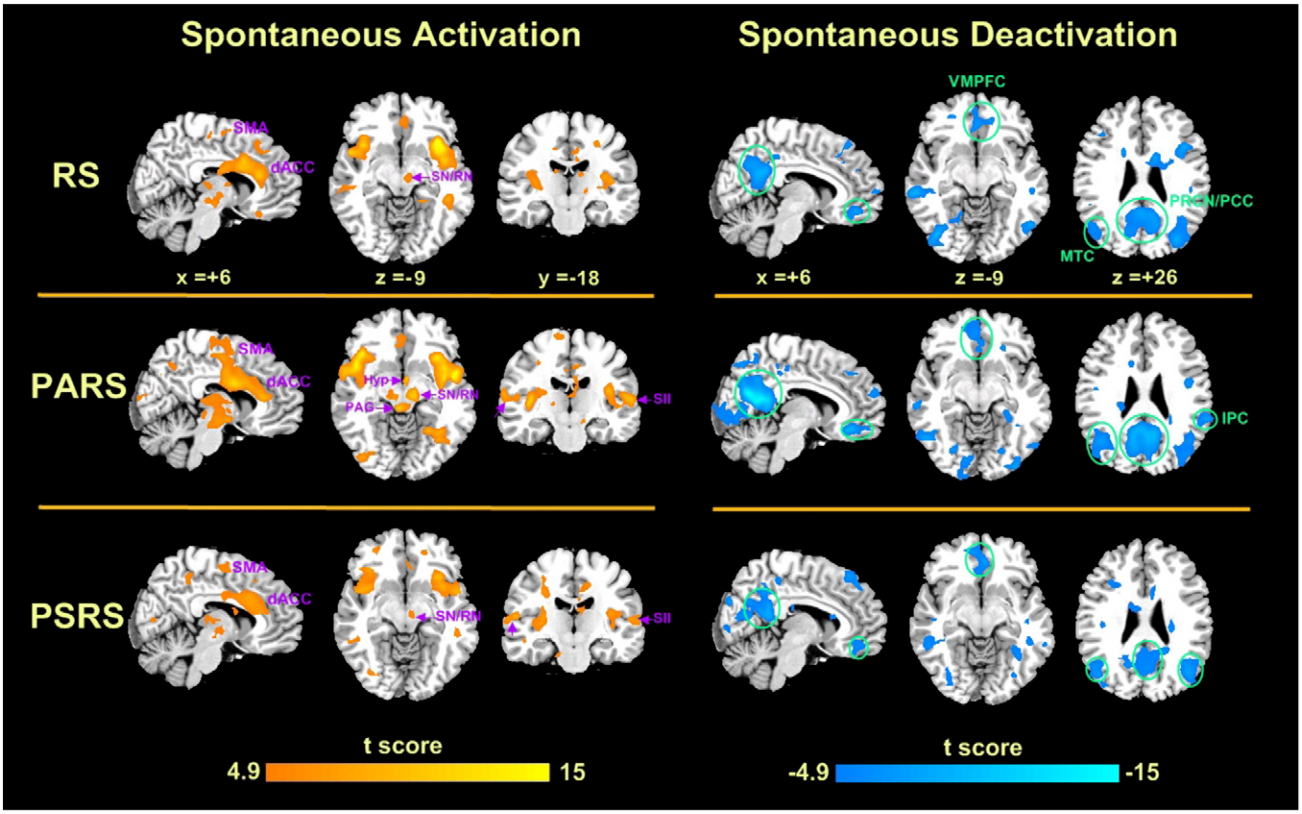

Fig. 2 – Neural networks associated with spontaneous activity in the right AI. During both RS, PARS and PSRS (N = 14), the right AI showed prominently spontaneous activations associated with the SN and CEN-related regions, including the insula, SMA, dACC, thalamus, and substantia nigra/RN (P < 0.005, FDR corrected, cluster size > 10 voxels). Conversely, the spontaneous deactivations were primarily distributed in the DMN network, such as PCC/PRCN, VMPFC, and MTC. Notably, the enhanced dichotomy of the anticorrelated CEN and DMN networks emerged particularly during the PARS.

stable (see in Fig. 2, $P<0.005$, FDR corrected, cluster size > 10 voxels). However, in comparison with RS, we also identified significant changes (both in spatial distributions and response magnitudes) during the PARS (see in Fig. 3 and Table 2, $P<0.01$, FDR corrected, cluster size > 10 voxels). There were prominently increased spontaneous activations within the CEN-related nuclei (DLPFC; SMA; posterior parietal cortex, PPC; secondary somatosensory cortex, SII), and enhanced deactivations in the core regions of the DMN network (the PCC/PRCN; IPC; MTC; MTL). Notably, the most modulated changes were exhibited in the SN network, particularly some paralimbic and subcortical regions (bilateral insula; dACC; hypothalamus, Hyp; thalamus; periaqueductal gray, PAG; substantia nigra/RN). Though increased spontaneous activations also emerged following the PSRS ($P<0.01$, FDR corrected, cluster size > 10), these regions were primarily limited to the CEN network (DLPFC, SMA and SII), and one SN-related region (dACC). Notably, the enhanced deactivation was only identified in the MTC. In addition, ACUP can enhance the spontaneous activations within the SN network (insula, Hyp, PAG and substantia nigra), and increase the spontaneous deactivations in the core regions of the DMN network (PCC/PRCN and medial temporal lobe of the amygdala), in comparison with the SHAM (shown in Fig. 3). The attenuation of both spontaneous activation and deactivation did not reach a statistical significance level for these three PARS vs. RS, PSRS vs. RS and PARS vs. PSRS comparisons ($P<0.01$, FDR corrected, cluster size > 10 voxels).

3. Discussion

Acupuncture has shown its promise in treating chronic pain and other disorders by mobilizing the neurophysiological system to modulate multisystem functions (Chang, 1982; Dhond et al., 2008; Ionescu-Tirgoviste et al., 1991). These vital functions may be typically delayed from the needle stimulation phase, and exert the sustained modulatory effect on the spontaneous coherences of the post-stimulus "resting" brain (Bai et al., 2009b; Dhond et al., 2008; Liu et al., in press; Qin et al., 2008; Zhang et al., 2009b). A series of papers using task-free, intrinsic connectivity analyses have already revealed the interplay of three canonical networks that existed in the intrinsic human brain: the SN and CEN network are inversely correlated with the DMN (Greicius et al., 2003; Greicius and Menon, 2004; Gusnard et al., 2001). Recently, some researchers extend this discovery, and suggest that the anterior insula, a key node in the SN, plays a central role in the hierarchical initiation of control signals, specifically with respect to activation and deactivation in the CEN and DMN (Sridharan et al., 2008). By adopting spontaneous activity

Table 2 – The right AI-associated both spontaneous activations and deactivations during the RS (df=13, P<0.005, FDR corrected, cluster size>10 voxels); paired t-test for PARS vs. RS, and PSRS vs. RS (df=13, P<0.01, FDR corrected, cluster size>10 voxels).

Spontaneous activation		RS					Paired t-test of PARS vs.RS					Paired t-test of PSRS vs.RS				
		Talairach			t value	Voxels	Talairach			t value	Voxels	Talairach			t value	Voxels
		x	y	z			x	y	z			x	y	z		
Interoceptive–autonomic related areas																
Insula	L	−39	20	2	12.8	237	−42	−3	6	8.8	124					
BA 13	R	33	20	6	13.5	402	44	−5	7	9.6	189					
dACC	L	−8	36	20	8.8	112	−8	38	17	4.8	55	−6	36	19	4.1	21
BA 24/32	R	5	23	24	9.6	143	5	24	25	5.3	58	5	32	23	4.3	27
Hypothalamus	R						3	−3	−7	5.2	12					
PAG	L						−3	−27	−8	5.4	14					
	R						3	−27	−8	5.6	11					
Substantia nigra/RN	L						−9	−14	−8	5.8	31					
	R	9	−19	−8	6.3	27	9	−15	−8	6.4	25					
Thalamus	L	−8	−26	7	7.5	33	−8	−26	9	5.4	79					
Central-executive related areas																
DLPFC	L	−46	40	24	5.7	11	−32	20	43	5.6	22	−46	5	31	4.0	11
BA 9/46	R						44	36	17	5.8	29	46	38	17	4.2	13
SMA (BA 6)	L	−2	−18	57	4.8	34	−1	−24	57	4.5	60	−1	−21	57	3.9	36
PPC (BA 7)	R						22	−48	65	4.8	51					
SII	L						−62	−22	20	6.1	34	−65	−17	15	6.3	22
BA 40/43	R						53	−28	18	6.3	42	62	−23	15	6.5	28
Spontaneous deactivation default mode related areas																
Default mode related areas																
PCC/PRCN	L	−7	−56	25	−6.7	363	−8	−57	23	−6.2	132					
BA 23/31	R	7	−51	25	−7.1	403	3	−45	25	−6.8	112					
VMPFC	L	−6	42	−8	−6.4	17										
BA 10	R	6	45	−9	−5.2	24										
Inferior parietal cortex	L						−46	−36	52	−4.2	34					
BA 40	R						55	−44	26	−4.9	47					
Medial Amygdala	R						24	−6	−15	−4.6	12					
temporal lobe PH/hipp (BA 34)	R						16	−6	−18	−4.9	17					
Medial temporal cortex	L	−44	−63	27	−4.3	90	−41	−61	27	−5.3	41					
BA 39	R	51	−63	29	−5.9	132						56	−63	27	−4.1	33

The coordination of voxel with the maximal signal change within each region was listed. During the RS, red color denoted the AI-related spontaneous activation, and blue for deactivation. During both PARS vs. RS and PSRS vs. RS, red and blue color indicated the increased AI-related spontaneous activation and deactivation respectively. No significance of attenuated spontaneous activity was found when comparing the PARS and PSRS with the RS.

Abbreviations: BA—Brodmann area; dACC—dorsal anterior cingulate cortex; PAG—periaqueductal gray; RN—red nucleus; DLPFC—dorsolateral prefrontal cortex; SMA—supplementary motor area; PPC—posterior parietal cortex; SII—secondary somatosensory cortex; PCC—posterior cingulate cortex; PRCN—precuneus; VMPFC—ventromedial prefrontal cortex; PH—parahippocampus; Hipp—hippocampus.

detection approach, the present study aimed to explore the way the sustained effect of acupuncture modulated these large-scale resting networks anchored by the anterior insula. Results indicated that the somatosensory stimulation (ACUP) can not only deepen the dichotomy of anticorrelated CEN and DMN networks, but also enhance the intrinsic coherences of interoceptive–autonomic areas within the SN. These findings may forge a new link between the intrinsic human brain connectivity and neural mechanisms underlying the sustained effects of acupuncture.

During the resting state, previous studies have demonstrated that the spontaneous fluctuations of blood oxygenation level-dependent (BOLD) signals are coherent within specific neuroanatomical systems in the human brain (Fox et al., 2005; Greicius et al., 2003). However, most studies adopted standard functional connectivity analysis, and primarily focused on the correlation patterns between different brain areas rather than on the activity pattern within a specific brain region. The spontaneous activity detection approach in the present study may provide a more direct evaluation of the characteristics of intrinsic coherence network, during the task-free resting state. Our findings showed that there were intermittent episodes of strikingly increased activity in the right AI when subjects were in the resting state. This strikingly increased activity, which exceeds the statistical definition of activity used in the analysis of fMRI data, can be defined as spontaneous activity (Hunter et al., 2006). For each subject, the spontaneous activity was not random in that they were distinctly clustered both temporally and spatially (see in Table 1); at the group level, about 5 time points (more than 10% of the total number) showed spontaneous activity and these activated time points included an average of 35 voxels

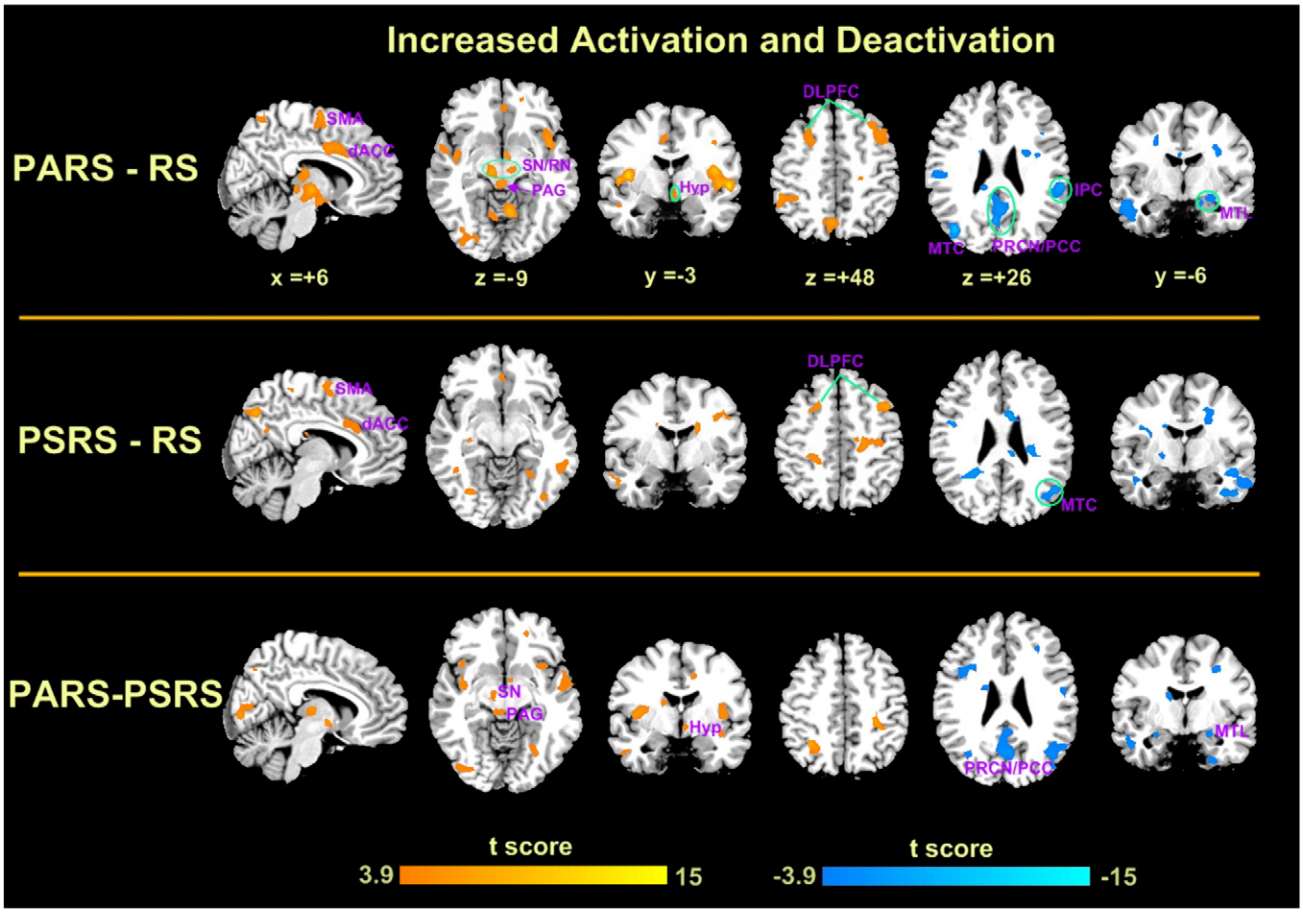

Fig. 3 – Modulated anticorrelated resting brain networks (SN, CEN and DMN) during the PARS and PSRS. During the PARS, there were prominently increased spontaneous activations in the CEN-related nuclei (SMA and DLPFC), and enhanced deactivations in the core regions of the DMN network (PCC/PRCN, IPC, MTC and MTL) ($P<0.01$, FDR corrected, cluster size > 10 voxels). Notably, the most significant changes were exhibited within the SN network, particular some paralimbic and subcortical regions (insula, dACC, Hyp, thalamus, PAG, and substantia nigra/RN). Though some increased spontaneous activation also emerged following the PSRS ($P<0.01$, FDR corrected, cluster size > 10 voxels), these regions were primarily limited to the CEN network (SMA and DLPFC), and one SN-related region (dACC). And the enhanced deactivation was only identified in the MTC. For the PARS, there were enhanced spontaneous activations within the SN network (insula, Hyp, PAG and substantia nigra), while there were deactivations in the core regions of the DMN network (PCC/PRCN and medial temporal lobe of the amygdala), in comparison with the PSRS.

(about 18% of the total number of voxels in the right AI), which greatly exceeded the statistically expected frequencies.

The functional distinction between internal and external processing has long been acknowledged by psychologists (Antrobus, 1968; Binder et al., 1999). They uphold that the brain is a system intrinsically operating on its own, primarily driven by internal dynamics, with external events modulating rather than determining the activity of the systems (Raichle and Gusnard, 2005; Raichle and Mintun, 2006). The basic organization of these resting networks was again corroborated by our results that there were prominently AI-related spontaneous activations distributed within the SN and CEN, and deactivations in the DMN. Even following the ACUP and SHAM, the organization of these resting networks maintained relatively stable (see in Fig. 2).

One fundamental mechanism underlying the alternating interplay between the exogenous and endogenous sources of the central processing is the control signal from the AI, which can thereby cause switching between the CEN and DMN networks (Sridharan et al., 2008). Following the external acupuncture intervention, we found that the dichotomy of these anticorrelated networks exhibited significant enhancements. The increased spontaneous activations anchored by the AI were presented in the CEN-related regions such as the DLPFC, PPC, SMA and SII (see in Fig. 3 and Table 2); in contrast, enhanced deactivations were primarily distributed in the core regions of the DMN network, including PCC/PRCN, IPC, MTC, and MTL (Amy and PH/Hipp). This phenomenon may be partially brought forth by the switching between the DMN and CEN when an external stimulus (i.e. acupuncture) was input. The CEN network is equipped to operate on such identified external changes, which requires directing attention to pertinent stimuli as behavioral choices are weighed against shifting conditions and background homeostatic demands

(Seeley et al., 2007). A network geared for this purpose should include known sites for sustained attention (DLPFC) (Curtis and D'Esposito, 2003), perceived intrusion or threat (PPC) (Price, 2002), nociceptive sensations (SII) (Tracey and Mantyh, 2007), and response selection (SMA) (Lau et al., 2006). This was why these increased spontaneous activations were also presented during the PSRS (see in Fig. 3 and Table 2). Meanwhile, the enhanced attenuations within the DMN may be consistent with the notion that these "deactivated" brain regions wax during task-free periods and wane during task performance (Raichle et al., 2001). Presumably these significant changes in spontaneous fluctuations, either ramping up or tapering off, may imply a reallocation of processing resources toward a stronger and more attentionally demanding stimulus (i.e. acupuncture), as there are finite brain resources available for information processing.

While some commonly altered intrinsic coherences emerged following both interventions, there were also increased AI-associated spontaneous deactivation only identified following the ACUP, rather than the SHAM (shown in Fig. 3). This tendency was particularly exhibited in the limbic system, such as the Amy and PH/Hipp. A number of human studies using various approaches have concluded that the AI is a limbic integration cortex for complex and preprocessed sensory information (Augustine, 1996). Both directly and indirectly, the AI becomes part of the central circuitry that could mediate affective responses to pain via connections with the amygdala and projections from the amygdala to the PH/Hipp (Manning and Mayer, 1995). These limbic-related cortical regions, located in the medial temporal lobe, primarily support the encoding of the affective–cognitive aspects of pain (Becerra and Borsook, 2006). Moreover, signal attenuation of the Amy and PH/Hipp evoked by the acute effect of acupuncture are also observed as correlated with the elevation of pain threshold in subjects (Zhang et al., 2003). All these evidence may converge with one notion that some pain-affective areas were desensitized due to the acupuncture modulation.

Another significant difference between these two interventions was presented within the SN, particularly the Hyp and brainstem nuclei (PAG and substantia nigra) (see in Fig. 3). These regions are considered to be important nodes in the descending antinociceptive pathway for the central nervous system (CNS) mechanism of acupuncture (Wu et al., 1999). It is also well known from animal studies that the AI is connected to both the Hyp and brainstem structures (Field et al., 2006), which provides the likelihood of finding a functional nociceptive link for the "top-down" influences (Dunckley et al., 2005; Hadjipavlou et al., 2006; Tracey, 2002). As the Hyp and several descending modulatory regions in the brainstem are either ascending homeostatic integration sites or descending autonomic premotor sites, it is possibly feasible that a specific link exists between pain, homeostasis, and interoception. Provided the right AI plays a central role in the interoceptive–autonomic processing, the observed AI-associated intrinsic coherences of the limbic and brainstem regions are consistent with their contributions to basic aspects of endogenous pain-modulation mechanisms, and may form the basis for the top-down regulation of acupuncture administration.

Acupoint specificity is a controversial issue and still lacks scientifically rigorous evidence. In this study, we focused on the sustained effect of acupuncture, rather than its acute effect. Results revealed that the ACUP intervention can produce a distinct modulatory effect on the spontaneous activities of the resting brain networks, compared with the SHAM. Though preliminary, this phenomenon may reflect a potential characterization of the specific neuro-modulatory mechanism underlying the acupuncture. In addition, a recent study has reported differences in resting-state brain functions of people with chronic pain in contrast with controls, and the authors propose that this difference in resting-state brain activity might reflect the cognitive and affective complications of chronic pain (Baliki et al., 2008). Along these lines, exploration of the alternating interplay between the external acupuncture intervention and the organization of resting-state networks, can not only help us better understand the long-term effects of pain on the brain, but also the potential benefits of acupuncture in pain treatments. This hypothesis needs further investigations in the altered and/or dysfunctional brain networks such as those in patients with chronic pain.

In summary, the present study provides credence that acupuncture can modulate the spatio-temporal extent of the spontaneous activities within the resting brain networks anchored by the AI, particularly the enhancement of the intrinsic coherence in the interoceptive–autonomic network (i.e., SN). Although the precise physiological processes supported by such networks remain to be elucidated, we infer that the suppression of pain-affective areas and the enhancement of top-down endogenous pain-modulation circuits may form a basis for acupuncture action. Moreover, by investigating sustained effects of acupuncture rather than immediate action of needle manipulation, our study may offer a new perspective for exploring the central action of acupuncture. Considering that the anterior insula is a network hub to initiate dynamic switching between distinct brain networks across stimulus modalities (Sridharan et al., 2008), the mapping of the AI-associated neural networks may help elucidate how acupuncture as an exogenous stimulation modulates the endogenous self-regulation of homeostatic control mechanisms.

4. Experimental procedures

4.1. *Subjects*

In order to reduce intersubject variabilities, all the participants were recruited from a group of 14 college students [7 male, ages of 21.4±1.3 (mean±SD) years old]. They were all right-handed and acupuncture naïve. Exclusion criteria included any neurological disorder, any medical disorder that would impact the central nervous system, any contraindications to a high magnetic field, as well as any past or current history of psychiatric disorder, substance abuse or treatment with psychiatric medications within the last month. All subjects gave written, informed consent after the experimental procedures had been fully explained, and all research procedures were approved by the West China Hospital Subcommittee on

Human Studies. The experiment was also conducted in accordance with the Declaration of Helsinki.

4.2. *Experimental design*

A muti-block paradigm is generally used in fMRI studies, which implicitly presumes the temporal intensity profiles of the certain event conforming to the "on–off" specifications. Since the acupuncture action is slow to develop and resolve (Beijing, 1980; Mayer, 2000), the temporal aspects of the BOLD response to acupuncture may violate the assumptions of the block-designed estimates. In addition, using several stimulation blocks in a short period of time, investigators may not be able to dissociate the long-lasting effects from other confounding changes, such as the effect of needle manipulation during the experiment (Zhang et al., 2009). In the current study, we adopted a new experimental paradigm, namely the non-repeated event-related fMRI (NRER-fMRI) design (Qin et al., 2008), to investigate such prolonged effects after acupuncture administration.

The experiment consisted of three functional runs. Resting-state (RS) run lasted 12.5 min (see Fig. 4). Both the ACUP and SHAM runs employed the NRER-fMRI design paradigm, incorporating 1.5 min needle manipulation, preceded by 1 min rest epoch and followed by 12.5 min rest (without acupuncture manipulation) scanning. All participants were not informed of the order in which these three runs would be performed, and were asked to remain relaxed without engaging in any mental tasks. To facilitate blinding, they were also instructed to keep their eyes closed to prevent from actually observing the procedures. According to participants' reports after the scanning, they affirmed keeping awake during the whole process. The presentation sequence of these three runs was randomized and balanced throughout the population, and every participant performed only one run in each day in order to eliminate potential long-lasting effect following acupuncture administration.

Acupuncture was performed at acupoint ST36 on the right leg (Zusanli, located four finger breadths below the lower margin of the patella and one finger breadth laterally from the anterior crest of the tibia). This is one of the most frequently used acupoints and proved to have various efficacy in the treatments of the gastric and intestinal diseases, and pain management in both humans and animals (Manheimer et al., 2006; Sato et al., 2002). Acupuncture stimulation was delivered using a sterile disposable 38 ga stainless steel acupuncture needle, 0.2 mm in diameter and 40 mm in length. The needle was inserted vertically to a depth of 2–3 cm, and

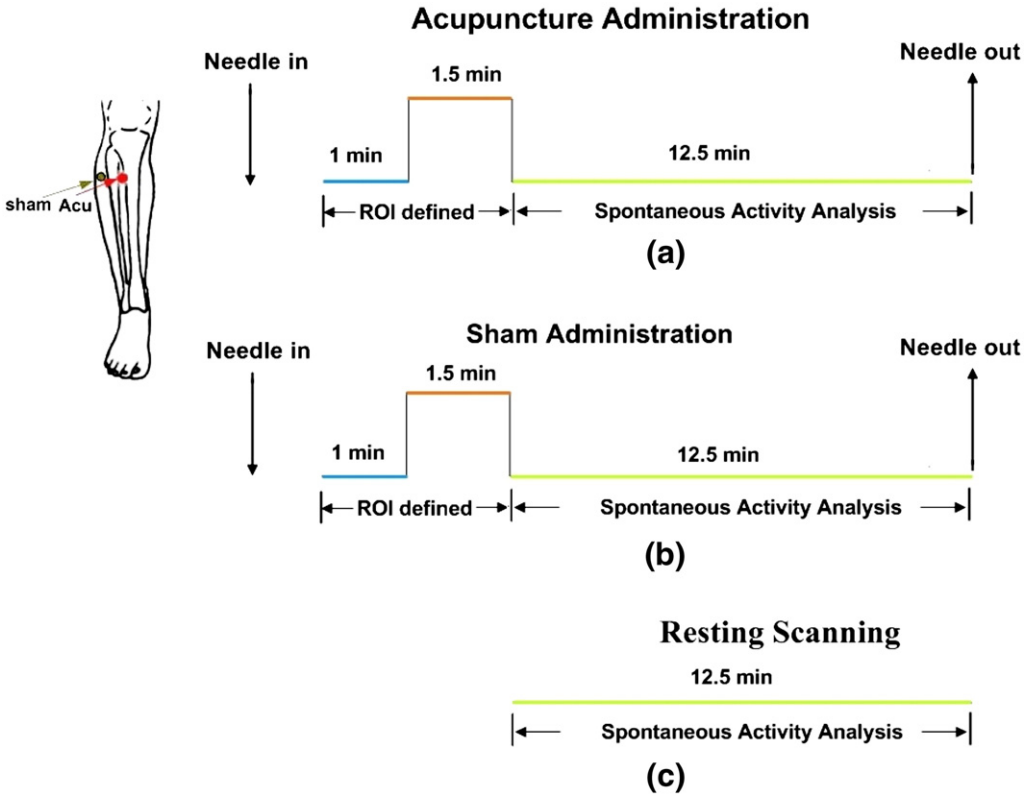

Fig. 4 – Experimental paradigm. Panel A indicated the verum acupuncture needle manipulation at acupoint ST 36 on the right leg (Zusanli, arrow pointing to red dot); Panel B presents the same design paradigm performed at a nonacupoint (2–3 cm apart from ST 36, arrow pointing to green dot); Panel C exhibits the 12.5 min resting-state scanning. For statistical analyses, the signal intensity during the 1-min rest phase (before stimulus) served as a control baseline for detecting the changes in signal intensity during acupuncture stimulation, thereby functionally defining the ROI. In addition, the data from the 12.5-min rest phase was used for further spontaneous activity detections. (For interpretation of the references to colour in this figure legend, the reader is referred to the web version of this article.)

administration was delivered by a balanced "tonifying and reducing" technique (Hui et al., 2000). Stimulation consisted of rotating the needle clockwise and counterclockwise for 1 min at a rate of 60 times per min. The procedure was performed by the same experienced and licensed acupuncturist on all participants.

Although the utility of the sham stimulation has been debated due to its lack of specificity, it was proved to be a reasonable placebo control in many acupuncture fMRI settings, and can effectively reduce the subjects' bias toward the stimulation (Li et al., 2003; Yoo et al., 2004). Here, we also employed the sham acupuncture as a control model. Sham acupuncture was initially devised by an experienced acupuncturist, with needling at nonmeridian points (2–3 cm apart from ST36) with needle depth, stimulation intensity, and manipulation method all identical to those used in the ACUP.

4.3. *Imaging data acquisition and analysis*

The MR images were acquired on a 3 T GE Signa scanner using a standard GE whole head coil (LX platform, gradients 40 mT/m, 150 T/m/s, GE Medical Systems, Milwaukee, Wisconsin). A custom-built head holder was used to prevent head movements. The images of 32 axial slices (FOV = 240 × 240 mm^2, matrix size = 64 × 64, slice thickness = 5 mm), parallel to the AC–PC plane and covering the whole brain, were acquired using a T2*-weighted single-shot, gradient-recalled echo planar imaging (EPI) sequence (TR = 1500 ms, TE = 30 ms, flip angle = 90°). Prior to the functional runs, high-resolution structural MR T1 images on each subject were acquired using a 3D sequence with a voxel size of 1 mm^3 for anatomical localization.

All preprocessing steps were carried out using statistical parametric mapping (SPM5, http://www.fil.ion.ucl.ac.uk/spm/). The images were first corrected for within-scan acquisition time differences between slices and then realigned to the first volume to correct for head motions (none of the subjects had head movements exceeding 1 mm on any axis and head rotation greater than one degree). The image data was further processed with spatial normalization based on the MNI space, re-sampled at 2 mm × 2 mm × 2 mm, and finally spatially smoothed with a 6 mm full-width-at-half maximum (FWHM) Gaussian kernel. Finally, the functional images were normalized to the Talairach stereotactic system (Talairach and Tournoux, 1998) and overlaid in MRIcro (http://www.sph.s.c.edu/comd/rorden/mricro.html) for presentation purposes.

4.4. *Psychophysical data collection and analysis*

As a concurrent psychophysical analysis, we used a verbal analog scale to ask participants to quantify the subjective sensations of acupuncture or *deqi* at the end of the ACUP and SHAM runs. The sensations are all listed on the MGH acupuncture sensation scale (MASS), including aching, soreness, pressure, heaviness, fullness, warmth, coolness, numbness, tingling, throbbing, dull or sharp pain and one blank row for subjects to add their own word(s) if the above descriptors did not embody the sensations they experienced during stimulation (Kong et al., 2007; Park et al., 2002). The intensity of each sensation was measured on a scale from 0 to 10 (0 = no sensation, 1–3 = mild, 4–6 = moderate, 7–8 = strong, 9 = severe and 10 = unbearable sensation). Since sharp pain was regarded to result from an inadvertent noxious stimulation rather than acupuncture *deqi* (Hui et al., 2005), we excluded the subjects for further analysis if they experienced sharp pain (greater than the mean by more than two standard deviations). In this cohort, none of subjects experienced the sharp pain. No subject opted to add an additional descriptor in the blank row provided.

In order to quantify the total intensity of *deqi* experienced by each individual, we employed the MASS index, defined as a weighted average of all sensations using an exponential smoothing (Kong et al., 2007). This index is convenient to devise a single value to quantitatively summarize the full multivariate breadth and depth of acupuncture sensations. In a further analysis, we compared the MASS index between these two stimulation (ACUP vs. SHAM) conditions using a paired *t*-test. By using Pearson correlation analysis, we also investigated the relation between the individual *deqi* composite (MASS index) and the activated voxel rate of brain regions.

4.5. *Definition of ROI*

Given that the post-stimulus period might still contain acupuncture-associated effects due to its long-acting characteristic, the mean signal intensity of the rest epoch preceded by the active stimulation served as a baseline. Then the difference in BOLD response between the stimulation and baseline condition was estimated on a voxel-by-voxel basis for each subject using the General Linear Model (GLM). This resulting contrast images for a single subject were then entered into the "random-effect" group analysis framework by one-sample *t*-test summary statistic ($P < 0.01$, FDR corrected). In ACUP and SHAM statistical parametric maps, the reliable activation within the insular cortex, common to both conditions, was located at the right anterior part (shown in Fig. 1C). A spherical ROI was defined as the set of voxels contained in 6 mm (in diameter) spheres centered on the peak of activation cluster within the overlapped right AI from the two stimulus conditions. This area was then used as the ROI for further spontaneous activity analyses (the ROI center's Talairach coordinates were 34, 22, 5; volume = 189 voxels with a peak *t*-score of 6.94).

Scaling and filtering were performed across all brain voxels (including those in the ROI) for the fMRI time series acquired during resting periods (RS, PARS, and PSRS) by the following two steps. (1) To minimize the effect of global drift, voxel intensities were scaled by dividing the value of each time point by the mean value of the whole-brain image at that time point. (2) The scaled waveform of each brain voxel was filtered using a bandpass filter ($\sim 0.008/s < f < \sim 0.1/s$) to reduce the effect of low-frequency drift and high-frequency noise (Lowe et al., 1998). Several sources of spurious or regionally nonspecific variance then were removed by regression including: six parameters obtained by rigid body head motion correction, the signal averaged over the whole brain, the signal averaged over the lateral ventricles, and the signal averaged over a region centered in the deep cerebral white matter (Fox et al., 2005).

4.6. Identification of spontaneous activations in the ROI

We used a procedure similar to Hunter et al. (2006) to identify the pattern of spontaneous activities in the right AI during both purely resting period and post-stimulus resting period respectively. To assure the independence of each time point in the analysis, we used 50 time points out of the total 500 time points (Desmond and Glover, 2002), with an interval of 10×1.5=15 s. For these 50 time points, the following procedures were applied to the ROI for each subject, based on both the height and spatial extent of signal changes:

(1) For each voxel, the Z value was calculated at each time point:

$$Z(t) = \frac{x(t) - mean(x)}{SD(x)},$$

Where x(t) was the signal value at the time point t, t=1, 2, 3… 50 and SD was the standard deviation.

(2) At each time point, the number of functionally defined voxels with Z>2 was calculated. Then the time points were ranked in a descending order of total voxels with Z>2. If the number of voxels with Z>2 at the first ranked time point exceeded 2.5% of the total voxel number in the ROI (i.e., exceeded the Gaussian assumptions), this time point was defined as a spontaneous activation time point (Spon-TP). Other time points were defined as the spontaneously activated time point only if they satisfied the following two criteria: (i) the number of voxels with Z>2 at this time point exceeded 2.5% of the total voxel number in the ROI. (ii) The voxels with Z>2 at this time point must be common to all higher-ranked time points that have been defined as Spon-TPs.

This approach utilizes both statistical height of activation (Z score) and extent of activation, i.e., a requirement that >2.5% of voxels exceed the height criterion. After detecting the spontaneously activated time point in the ROI, we obtained the time points of spontaneous activity ("Spon-TPs") and time points of no such activity ("Remain-TPs") for each subject.

4.7. Identification of brain networks associated with spontaneous activities in the right AI

The following procedures were also performed in SPM5. For each subject, the difference in BOLD signal between the Spon-TPs and Remain-TPs was estimated on a voxel-by-voxel basis throughout the entire brain. For each effect of interest, the relevant individual subject's contrast images from the first-level analyses were input as data points in a one-sample t-test, which were associated with spontaneous activities in the right AI at the group level. Finally, we obtained the AI-associated spontaneous networks under different conditions: RS, PARS and PSRS, respectively ($P<0.005$, FDR corrected). Here, we primarily focused on the modulatory effect of ACUP (or SHAM) on the resting-state spontaneous activities anchored by the right AI, and then we conducted the paired t-test to further identify differences in the spatial extent for the two comparisons, i.e., PARS vs. RS and PSRS vs. RS ($P<0.01$, FDR corrected).

4.8. Analyses of spontaneous deactivation

For identifying spontaneous deactivation during different conditions, we conducted the main analysis procedure substituting Z<−2 for Z>2 (Hunter et al., 2006). The Z score distribution across the entire brain presented significant voxels achieving Z<−2 exceeding the threshold expected under Gaussian distributions for these three conditions, PARS, PSRS and RS. Similarly, we performed the paired t-test to determine differences of spontaneous deactivation networks for PARS vs. RS, PSRS vs. RS and PARS vs. PSRS.

Acknowledgments

The authors thank Dr. Qiyong Gong and research staff at the West China Hospital who helped with experimentation and data collection. This paper is supported by Changjiang Scholars and Innovative Research Team in University (PCSIRT) under Grant No.IRT0645, Chair Professors of Cheung Kong Scholars Program, CAS Hundred Talents Program, the Joint Research Fund for Overseas Chinese Young Scholars under Grant No.30528027, the National Natural Science Foundation of China under Grant Nos. 30873462, 90209008, 30870685, 30672690, 30600151, 60532050, 60621001, the Beijing Natural Science Fund under Grant No. 4071003, the Project for the National Key Basic Research and Development Program (973) under Grant No.2006CB705700, 863 program under Grant No. 2008AA01Z411, and NIH under Grant No. NS45518, USA.

REFERENCES

Al-Sadi, M., Newman, B., Julious, S.A., 1997. Acupuncture in the prevention of postoperative nausea and vomiting. Anaesthesia 52, 658–661.

Antrobus, J.S., 1968. Information theory and stimulus-independent thought. Br. J. Psychol. 59, 423–430.

Augustine, J.R., 1996. Circuitry and functional aspects of the insular lobe in primates including humans. Brain Res. Rev 22, 229–244.

Bai, L., Qin, W., Tian, J., Liu, P., Li, L., Chen, P., Dai, J., Craggs, J.G., Deneen, K., Liu, Y., 2009a. Time-varied characteristics of acupuncture effects in fMRI studies. Hum. Brain Mapp. doi:10.1002/hbm.20769.

Bai, L., Qin, W., Tian, J., Dai, J., Yang, W., 2009b. Detection of dynamic brain networks modulated by acupuncture using a graph theory model. Prog. Nat. Sci. doi:10.1016/j.pnsc.2008.09.009.

Baliki, M.N., Geha, P.Y., Apkarian, A.V., Chialvo, D.R., 2008. Beyond feeling: chronic pain hurts the brain, disrupting the default-mode network dynamics. J. Neurosci. 28, 1398–1403.

Becerra, L., Borsook, D., 2006. Insights into pain mechanisms through functional MRI. Drug Discov. Today: Dis. Mech. 3, 313–318.

Beijing, S., 1980. Nanjing Colleges of Traditional Chinese Medicine. Essentials of Chinese Acupuncture. Foreign Language Press, Beijing.

Binder, J.R., Frost, J.A., Hammeke, T.A., Bellgowan, P.S., Rao, S.M., Cox, R.W., 1999. Conceptual processing during the conscious resting state: a functional MRI study. J. Cogn. Neurosci. 11, 80–95.

Birch, S., Hesselink, J.K., Jonkman, F.A., Hekker, T.A., Bos, A., 2004. Clinical research on acupuncture. Part 1. What have reviews of

the efficacy and safety of acupuncture told us so far? J. Altern. Complement. Med. 10, 468–480.
Bunge, S.A., Ochsner, K.N., Desmond, J.E., Glover, G.H., Gabrieli, J.D. E., 2001. Prefrontal regions involved in keeping information in and out of mind. Brain 124, 2074–2086.
Chang, H.T., 1982. Roles of acupuncture in medicine. Am. J. Chin. Med. 10, 1–4.
Craig, A.D., 2002. How do you feel? Interoception: the sense of the physiological condition of the body. Nat. Rev. Neurosci. 3, 655–666.
Craig, A.D., 2003. Interoception: the sense of the physiological condition of the body. Curr. Opin. Neurobiol. 13, 500–505.
Critchley, H.D., Wiens, S., Rotshtein, P., hman, A., Dolan, R.J., 2004. Neural systems supporting interoceptive awareness. Nat. Neurosci. 7, 189–195.
Curtis, C.E., D'Esposito, M., 2003. Persistent activity in the prefrontal cortex during working memory. Trends Cogn. Sci 7, 415–423.
Desmond, J.E., Glover, G.H., 2002. Estimating sample size in functional MRI (fMRI) neuroimaging studies: statistical power analyses. J. Neurosci. Meth. 118, 115–128.
Dhond, R.P., Yeh, C., Park, K., Kettner, N., Napadow, V., 2008. Acupuncture modulates resting state connectivity in default and sensorimotor brain networks. Pain 136, 407–418.
Diehl, D.L., 1999. Acupuncture for gastrointestinal and hepatobiliary disorders. J. Altern. Complement. Med. 5, 27–45.
Dunckley, P., Wise, R.G., Aziz, Q., Painter, D., Brooks, J., Tracey, I., Chang, L., 2005. Cortical processing of visceral and somatic stimulation: differentiating pain intensity from unpleasantness. Neuroscience 133, 533–542.
Fang, J., Jin, Z., Wang, Y., Li, K., Kong, J., Nixon, E.E., Zeng, Y., Ren, Y., Tong, H., Wang, Y., Wang, P., Hui, K.K., In Press. The salient characteristics of the central effects of acupuncture needling: limbic–paralimbic–neocortical network modulation. Hum. Brain Mapp.
Field, H.L., Basbaum, A.I., Heinricher, M.M., 2006. Central nervous system mechanisms of pain modulation. In: McMahon, S.B., Koltzenburg, M. (Eds.), Wall and Melzack's Textbook of Pain. InChurchill Livingstone, New York, pp. 125–142.
Fox, M.D., Snyder, A.Z., Vincent, J.L., Corbetta, M., Van Essen, D.C., Raichle, M.E., 2005. The human brain is intrinsically organized into dynamic, anticorrelated functional networks. Proc. Natl. Acad. Sci. U. S. A. 102, 9673–9678.
Greicius, M.D., Krasnow, B., Reiss, A.L., Menon, V., 2003. Functional connectivity in the resting brain: a network analysis of the default mode hypothesis. Proc. Natl. Acad. Sci. U. S. A. 100, 253–258.
Gusnard, D.A., Raichle, M.E., Raichle, M.E., 2001. Searching for a baseline: functional imaging and the resting human brain. Nat. Rev. Neurosci. 2, 685–694.
Greicius, M.D., Menon, V., 2004. Default-mode activity during a passive sensory task: uncoupled from deactivation but impacting activation. J. Cognitive Neurosci. 16, 1484–1492.
Hadjipavlou, G., Dunckley, P., Behrens, T.E., Tracey, I., 2006. Determining anatomical connectivities between cortical and brainstem pain processing regions in humans: a diffusion tensor imaging study in healthy controls. Pain 123, 169–178.
Han, J.S., Terenius, L., 1982. Neurochemical basis of acupuncture analgesia. Annu. Rev. Pharmacol. Toxicol. 22, 193–220.
Hui, K.K., Liu, J., Makris, N., Gollub, R.L., Chen, A.J., Moore, C.I., Kennedy, D.N., Rosen, B.R., Kwong, K.K., 2000. Acupuncture modulates the limbic system and subcortical gray structures of the human brain: evidence from fMRI studies in normal subjects. Hum. Brain Mapp. 9, 13–25.
Hui, K.K.S., Liu, J., Marina, O., Napadow, V., Haselgrove, C., Kwong, K.K., Kennedy, D.N., Makris, N., 2005. The integrated response of the human cerebro-cerebellar and limbic systems to acupuncture stimulation at ST36 as evidenced by fMRI. Neuroimage 27, 479–496.
Hunter, M.D., Eickhoff, S.B., Miller, T.W.R., Farrow, T.F.D., Wilkinson, I.D., Woodruff, P.W.R., 2006. Neural activity in speech-sensitive auditory cortex during silence. Proc. Natl. Acad. Sci. U. S. A. 103, 189–194.
Ionescu-Tirgoviste, C., Pruna, S., Bajenaru, O., 1991. The participation of the autonomic nervous system in the mechanism of action of acupuncture. Am. J. Acupunct. 19, 21–28.
Koechlin, E., Summerfield, C., 2007. An information theoretical approach to prefrontal executive function. Trends Cogn. Sci 11, 229–235.
Kong, J., Ma, L., Gollub, R.L., Wei, J., Yang, X., Li, D., Weng, X., Jia, F., Wang, C., Li, F., 2002. A pilot study of functional magnetic resonance imaging of the brain during manual and electroacupuncture stimulation of acupuncture point (LI-4 Hegu) in normal subjects reveals differential brain activation between methods. J. Altern. Complement. Med. 8, 411–419.
Kong, J., Gollub, R., Huang, T., Polich, G., Napadow, V., Hui, K., Vangel, M., Rosen, B., Kaptchuk, T.J., 2007. Acupuncture de qi, from qualitative history to quantitative measurement. J Altern. Complement. Med. 13, 1059–1070.
Kwon, Y.D., Pittler, M.H., Ernst, E., 2006. Acupuncture for peripheral joint osteoarthritis: a systematic review and meta-analysis. Rheumatology (Oxford) 45, 1331–1337.
Lau, H., Rogers, R.D., Passingham, R.E., 2006. Dissociating response selection and conflict in the medial frontal surface. Neuroimage 29, 446–451.
Li, G., Liu, H.L., Cheung, R.T.F., Hung, Y.C., Wong, K.K.K., Shen, G.G. X., Ma, Q.Y., Yang, E.S., 2003. An fMRI study comparing brain activation between word generation and electrical stimulation of language-implicated acupoints. Hum. Brain Mapp. 18, 233–238.
Liu, P., Qin, W., Zhang, Y., Tian, J., Bai, L., Zhou, G., Liu, J., Chen, P., Dai, J., in press. Combining spatial and temporal information to explore function-guide action of acupuncture using fMRI. J. Magn. Reson. Imag.
Lowe, M.J., Mock, B.J., Sorenson, J.A., 1998. Functional connectivity in single and multislice echoplanar imaging using resting-state fluctuations. Neuroimage 7, 119–132.
Manheimer, E., Lim, B., Lao, L., Berman, B., 2006. Acupuncture for knee osteoarthritis—a randomised trial using a novel sham. Acupunct. Med. 24, 7–14.
Manning, B.H., Mayer, D.J., 1995. The central nucleus of the amygdala contributes to the production of morphine antinociception in the rat tail-flick test. J. Neurosci. 15, 8199–8213.
Mayer, D.J., 2000. Acupuncture: an evidence-based review of the clinical literature. Anal. Rev. Med. 51, 49–63.
Mesulam, M.M., Mufson, E.J., 1982. Insula of the old world monkey. III: Efferent cortical output and comments on function. J. Comp. Neurol. 212, 38–52.
Mufson, E.J., Mesulam, M.M., 1982. Insula of the old world monkey. II: Afferent cortical input and comments on the claustrum. J. Comp. Neurol. 212, 23–37.
NIH, 1998. NIH Consensus Conference. Acupunct. Jama 280, 1518–1524.
Park, H., Park, J., Lee, H., Lee, H., 2002. Does deqi (needle sensation) exist? Am. J. Chinese Med. 30, 45–50.
Price, D.D., Rafii, A., Watkins, L.R., Buckingham, B., 1984. A psychophysical analysis of acupuncture analgesia. Pain 19, 27–42.
Price, D.D., 2002. Central neural mechanisms that interrelate sensory and affective dimensions of pain. Mol. Interv. 2, 392–403.
Qin, W., Tian, J., Bai, L., Pan, X., Yang, L., Chen, P., Dai, J., Ai, L., Zhao, B., Gong, Q., 2008. FMRI connectivity analysis of

acupuncture effects on an amygdala-associated brain network. Mol. Pain 4, 55–71.
Raichle, M.E., MacLeod, A.M., Snyder, A.Z., Powers, W.J., Gusnard, D.A., Shulman, G.L., 2001. Inaugural article: a default mode of brain function. Proc. Natl. Acad. Sci. U. S. A. 98, 676–682.
Raichle, M.E., Gusnard, D.A., 2005. Intrinsic brain activity sets the stage for expression of motivated behavior. J. Comp. Neurol. 493, 167–176.
Raichle, M.E., Mintun, M.A., 2006. Brain work and brain imaging. Annu. Rev. Neurosci. 29, 449–476.
Sato, A., Sato, Y., Uchida, S., 2002. Reflex modulation of visceral functions by acupuncture-like stimulation in anesthetized rats. Int. Cong. Ser. 1238, 111–123.
Seeley, W.W., Menon, V., Schatzberg, A.F., Keller, J., Glover, G.H., Kenna, H., Reiss, A.L., Greicius, M.D., 2007. Dissociable intrinsic connectivity networks for salience processing and executive control. J. Neurosci. 27, 2349–2356.
Sridharan, D., Levitin, D.J., Menon, V., 2008. A critical role for the right fronto-insular cortex in switching between central-executive and default-mode networks. Proc. Natl. Acad. Sci. U. S. A. 105, 12569–12574.
Takeda, W., Wessel, J., 1994. Acupuncture for the treatment of pain of osteoarthritic knees. Arthritis Care Res. 7, 118–122.
Talairach, J., Tournoux, P., 1998. Co-planar Stereotaxic Atlas of the Human Brain. Thieme Medical Publishers, New York.
Tracey, I., Mantyh, P.W., 2007. The cerebral signature for pain perception and its modulation. Neuron 55, 377–391.
Tracey, K.J., 2002. The inflammatory reflex. Nature 420, 853–859.
Witt, C., Brinkhaus, B., Jena, S., Linde, K., Streng, A., Wagenpfeil, S., Hummelsberger, J., Walther, H.U., Melchart, D., Willich, S.N., 2005. Acupuncture in patients with osteoarthritis of the knee: a randomised trial. Lancet 366, 136–143.
Worsley, K.J., Friston, K.J., 1995. Analysis of fMRI time-series revisited—again. Neuroimage 2, 173–181.
Wu, M.T., Hsieh, J.C., Xiong, J., Yang, C.F., Pan, H.B., Chen, Y.C., Tsai, G., Rosen, B.R., Kwong, K.K., 1999. Central nervous pathway for acupuncture stimulation: localization of processing with functional MR imaging of the brain-preliminary experience. Radiology 212, 133–141.
Yoo, S.S., Teh, E.K., Blinder, R.A., Jolesz, F.A., 2004. Modulation of cerebellar activities by acupuncture stimulation: evidence from fMRI study. Neuroimage 22, 932–940.
Zhang, W.T., Jin, Z., Cui, G.H., Zhang, K.L., Zhang, L., Zeng, Y.W., Luo, F., Chen, A.C.N., Han, J.S., 2003. Relations between brain network activation and analgesic effect induced by low vs. high frequency electrical acupoint stimulation in different subjects: a functional magnetic resonance imaging study. Brain Res. 982, 168–178.
Zhang, Y., Qin, W., Liu, P., Tian, J., Liang, J.M., Deneen, K.M., Liu, Y.J., 2009a. An fMRI study of acupuncture using independent component analysis. Neurosci. Lett. 449, 6–9.
Zhang, Y., Liang, J., Qin, W., Liu, P., Deneen, K., Chen, P., Bai, L., Tian, J., Liu, Y., 2009b. Comparison of visual cortical activations included by electro-acupuncture at vision and nonvision-related acupoints. Neurosci. Lett. 458, 6–10.